Transport Properties of Surface-Modified Single-Walled Carbon Nanotubes

Denys O. Shpylka, Iryna V. Ovsiienko, Tetiana A. Len, Lyudmila Yu. Matzui, Yuriy I. Prylutskyy, Ilgar Mirzoiev, and Tatiana L. Tsaregradskaya

Abstract The paper presents the results of studies of transport properties of single-walled carbon nanotubes modified with cobalt-containing complexes. It is revealed that for source single-walled carbon nanotubes the main mechanism of conductivity is the hopping conductivity with the variable hopping length for 3D system. Magnetoresistance of as-sprepared carbon nanotubes is caused by two mechanisms, such as mechanism of compression of the wave function of localized charge carriers and spin-orbital mechanism. The thermopower of as-prepared SWCNTs is linearly dependent on temperature. It is shown that modification of single-walled carbon nanotubes by cobalt-containing complexes results into a change in the character of the conductivity for bulk specimens of single-walled carbon nanotubes. For bulk specimens of modified single-walled carbon nanotubes conductivity is described in the terms of power temperature law that is typical for individual single-walled carbon nanotubes. The negative magnetoresistance observed for modified SWCNTs at low temperatures is related with the manifestation of the effect of charge carriers' weak localization for a one-dimensional system. Thermopower of modified carbon nanotubes is the sum of the diffuse and phonon drag components of thermopower.

1 Introduction

Investigations of the single-walled carbon nanotubes (SWCNTs) have attracted much interest due to their unique properties and great application potentials . One of

D. O. Shpylka (✉) · I. V. Ovsiienko · T. A. Len · L. Yu. Matzui · T. L. Tsaregradskaya
Departments of Physics, Taras Shevchenko National University of Kyiv, Volodymyrska 64/13, Kyiv 01601, Ukraine
e-mail: denys8600@ukr.net

Y. I. Prylutskyy
Departments of Biophysics, Taras Shevchenko National University of Kyiv, Volodymyrska 64/13, Kyiv 01601, Ukraine

I. Mirzoiev
B. Verkin Institute for Low Temperature Physics and Engineering of NAS of Ukraine, Nauky Ave. 47, Kharkiv 61103, Ukraine

O. Fesenko and L. Yatsenko (eds.), *Nanostructured Surfaces, Nanocomposites and Nanomaterials, and Their Applications*, Springer Proceedings in Physics 296,
https://doi.org/10.1007/978-3-031-42704-6_5

the many aspects of investigations of SWCNTs is the study of the possibilities of changing their properties through surface functionalization and modification [1–5]. On the one hand, functionalization is a necessary step providing the formation of homogeneous dispersion of SWCNTs in solvents and, on the other hand, causes a significant number of defects in SWCNTs structure.

Another important direction of SWCNTs chemistry is chemical functionalization of SWCNTs with metal-containing molecular complexes. Such functionalization process not only opens the area of metal–organic chemistry to nanotubes, but also suggests potential applications in catalysis and molecular electronics.

A significant number of works is devoted to the issues of covalent and non-covalent functionalization of CNTs by metal-containing complexes [6–8]. In these papers methods for obtaining such complexes on the surface of CNTs and their properties are considered. Thus, the effect of the surface functionalization with complexes containing magnetic metals on the magnetic properties of CNTs has been theoretically considered in [9]. In [10] influence of surface functionalization with transition-metal phthalocyanines on reduction ability has been studied. The main focus in the articles is paid to the chemical properties of the obtained modified CNTs, in particular chemical stability of functionalized SWCNTs [11], their catalytic activity and the possibility of using them as catalysts in chemical synthesis [11, 12], increasing the solubility of SWCNTs in various solvents and the possibility of forming colloidal solutions and dispersions of CNTs [13]. However, the questions of changing the physical properties of modified on the surface with metal-containing complexes SWCNTs, especially the properties associated with charge transfer, are discussed in these works much less. This especially applies to experimental studies of the properties of functionalized CNTs.

The main goal of presented work is to establish the possibility of surface modification of SWCNTs by cobalt-containing complexes, to identify the structural and morphological state of cobalt on the surface of SWCNTs, as well as to study the influence of surface modification on the transport properties of bulk specimens of modified SWCNTs.

2 Experimental

2.1 As-Prepared Carbon Nanotubes

As source for modification single carbon nanotubes (as-prepared SWCTs) have been chosen. As-prepared SWCNTs with mean value of tubes diameter ~ 1.4 nm have been produced by catalytic decomposition of acetylene with use yttrium and nickel as catalysts.

Figure 1 presents the fragment of X-ray diffraction pattern for as-prepared SWCTs.

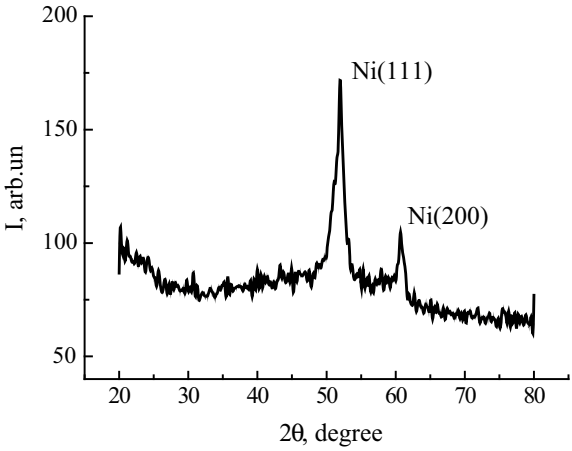

Fig. 1 Fragment of X-ray diffraction pattern for as-prepared SWCTs

As can be seen from the figure the X-ray diffraction pattern contains only intensive peaks that correspond to nickel. The graphite lines are absent on the diffractogram. Thus, there are no ordered multi-walled carbon structures in the source nanocarbon material.

The fragment of transmission electron microscopy image of as-prepared SWCNTs is presented in Fig. 2.

As it is seen from the figure long strands from 3 nm up to 8 nm in diameter, which apparently consist of thinner CNTs, as well as catalyst metal particles and disordered carbon particles up to 5 nm in size, are visualized in the image.

The presence of nanosized nickel particles is also confirmed by the results of thermo-magnetometric studies, which are presented in Fig. 3.

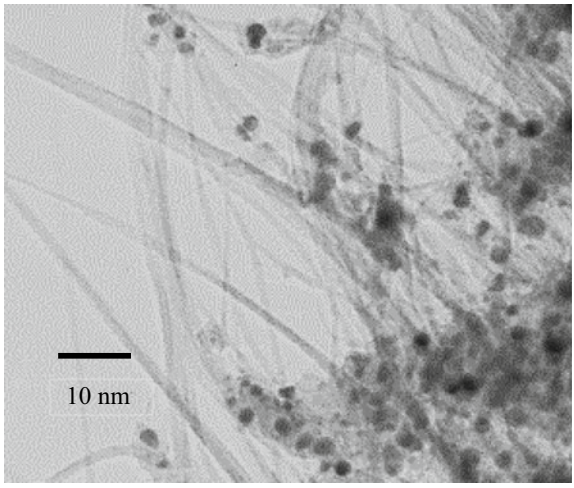

Fig. 2 Fragment of TEM image of as-prepared SWCNTs

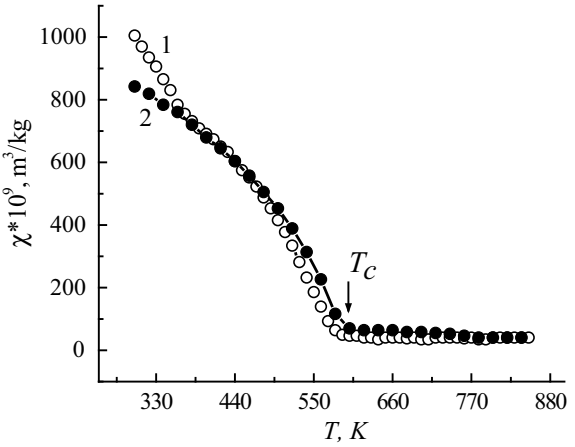

Fig. 3 Temperature dependence of magnetic susceptibility $\chi(T)$ for as-prepared SWCNTs

As it follows from the figure, character of temperature dependence $\chi(T)$ for as-prepared SWCNTs is typical as for material containing magnetic admixture nickel. However, the Curie temperature according to the experimental results is slightly shifted toward low temperatures $T_C = 580$ K in comparison with the Curie temperature for bulk nickel ($T_{Cb} = 630$ K).

Such shifting of Curie point can be explained by nanodispersive character of nickel particles distribution.

Estimating the size L of nickel particles according to [14]

$$L = 3d\left[\frac{T_C}{2(T_{Cb} - T_C)} - 1\right], \tag{1}$$

where d is the atomic or molecular diameter of magnetic phase, gives a value of $L \sim$ 2.2 nm, which correlates well with the size of the catalyst metal particles according to electron microscopy data.

Thus, the source for modification as-prepared SWCNTs is nanocarbon material containing only SWCNTs in the form of strands and separate tubes and some portion of the metal catalyst in the form of nanosized particles.

2.2 Modification of Source SWCNTs

The chemical modification of as-prepared SWCNTs has been carried out in four stages.

At the first stage, the tubes were opened from the ends (the «caps» on the ends of tubes were torn off) and cut into smaller pieces, i.e., the size and structure of the tubes changed. For this, the as-prepared SWCNTs were treated with a 35% aqueous solution of hydrogen peroxide for 18 h.

The task of the second stage of processing was to remove metal catalyst residues from the as-prepared SWCNTs. For this, the as-prepared SWCNTs were boiled in a hydrochloric acid solution for 10 h, after which the water-soluble nickel chloride was washed out.

At the third stage, the SWCNTs surface was functionalized to create conditions for attachment of cobalt cations to the tubes surface, since cobalt cations cannot directly attach to the SWCNTs surface. Non-covalent functionalization was carried out with three different surfactants: 1,3diaminopropane (DAP, specimen #1), monoethanolamine (MEA, specimen #2) and 1,3diaminopropane in combination with benzophenone (specimen #3).

And at the last stage treated SWCNTs were heated at temperature 60 °C in cobalt (II) chloride solution, while the cobalt cations were attached through functional groups to the surface of the SWCNTs.

Thus, three specimens of modified SWCNTs which differ in the substance used to functionalize the surface were obtained.

2.3 *The Structure and Phase Composition of Modified SWCNTs*

The X-ray diffraction, tunnel electron microscopic and thermo-magnetometric investigations of modified SWCNTs have been carried out for definition of structure and phase composition.

Figure 4 presents the fragments of X-ray diffraction patterns for specimens of modified with different methods SWCNTs.

As it is follows from the figure none of the fragments of diffractograms for different specimens contain bands that correspond to reflections from graphite planes. Also, reflections corresponded to cobalt were not detected at the X-ray diffraction patterns.

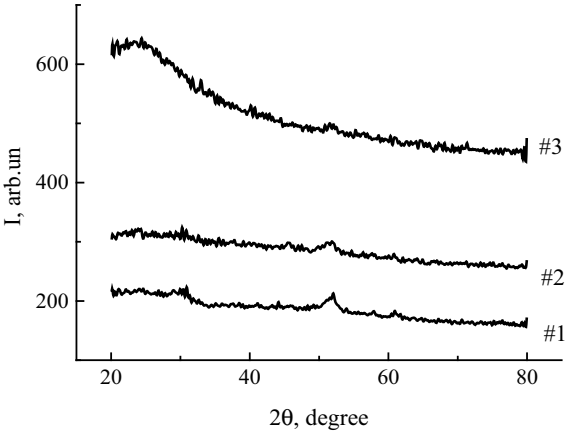

Fig. 4 Fragments of the X-ray diffraction patterns for specimens of modified SWCNTs. The specimen number is indicated in the figure

But all diffractograms contain weak bands, which can be detected as reflections from nickel catalyst.

The most intensive nickel line is observed for specimen #1; for specimen #3 the intensity of the nickel band is the weakest.

Thus, all specimens of modified SWCNTs do not contain any multilayer carbon structures and cobalt particles large than 0.3 nm. However, the cleaning methods that were used in the above schemes do not lead to the total deleting of the metal catalysts particles. Therefore, specimens of modified SWCNTs may contain small amounts of metal catalyst residues.

The fragment of TEM image of modified SWCNTs (specimen #1) is shown in Fig. 5.

As can be seen from the figure the chemical treatment of as-prepared SWCNTs results into separation of CNTs bunches into individual tubes and their shortening. Also, a significant decrease in the number of catalyst metal particles and disordered carbon particles is also observed.

The sizes of the remaining particles became significantly smaller compared to the source material.

Figure 6 shows the temperature dependences of magnetic susceptibility for modified with cobalt-containing complexes SWCNTs (specimen #1) for the alternating heating/cooling cycles.

As can be seen from the figure, the dependence $\chi(T)$ is very complicated. This complexity of dependence $\chi(T)$ reflects these complex processes that occur in the modified material during heating.

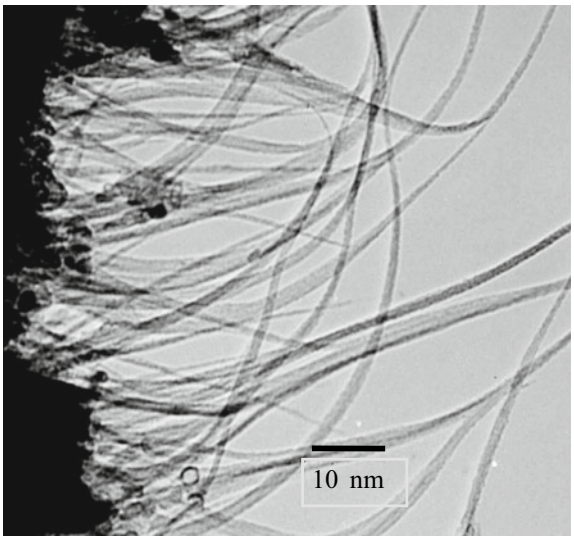

Fig. 5 Fragment of TEM image of modified by cobalt-containing complexes SWCNTs (specimen #1)

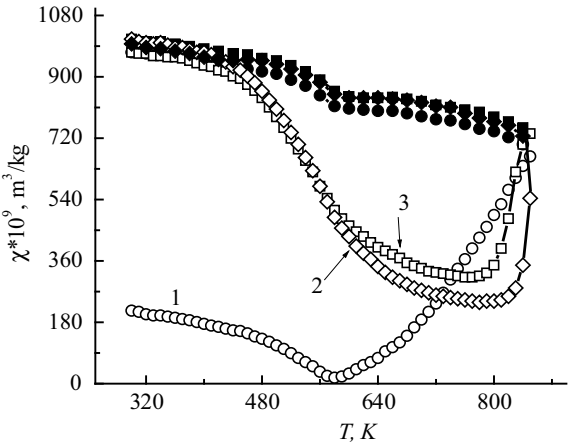

Fig. 6 Temperature dependences of magnetic susceptibility $\chi(T)$ for modified by cobalt-containing complexes SWCNTs (specimen #1) for the sequenced heating–cooling cycles, the curve number corresponds to the cycle number, the open labels are heating, and the closed ones are cooling

In the first heating cycle at a temperature of ~ 580 K, there is a minimum in the dependence, which is obviously associated with the transition from the ferromagnetic to the paramagnetic state of the remaining particles of the catalyst nickel, which, according to the X-ray diffraction data, is contained in small amounts in the modified SWCNTs.

Note that the transition temperature for modified SWCNTs coincides with the transition temperature for the as-prepared SWCNTs; however, the susceptibility value for the as-prepared SWCNTs below the Curie temperature is 6 times greater than for modified SWCNTs in the same temperature range. Upon further heating of the modified SWCNTs, the magnetic susceptibility begins to increase, which is uncharacteristic for a substance in a paramagnetic state. Such dependence $\chi(T)$ can be explained as follows. Cobalt, which is contained in modified SWCNTs as a cation in the composition of complex metal ion complexes and does not affect the magnetic state of the modified SWCNTs at temperatures below 580 K, begins to be reduced to pure cobalt when the temperature increases above 580 K. Small cobalt particles form large conglomerates as a result of thermally stimulated diffusion. This leads to a significant increase in the value of susceptibility since cobalt is a ferromagnet at temperatures up to 1388 K. When the specimen of modified SWCNTs is cooled, the value of the susceptibility practically does not change, and at a temperature of 580 K there is a weak jump in dependence $\chi(T)$. In more detail, the structural and phase composition of modified by cobalt-containing complexes SWCNTs is described in [15].

2.4 Methods of Measuring Transport Properties of Bulk

For measurement of transport properties, the bulk specimens from source and modified SWCNTs powders have been prepared by cold compacting without binder. The specimens are in the form of a rectangular parallelepiped with dimensions of 2 mm $\times$ 3.5 mm $\times$ 15 mm and density up to 1.6 g/cm^3. In the bulk specimens there is a prevailing orientation of CNTs so that the axes of CNTs lie in a plane perpendicular to the pressure direction.

Electrical resistance of bulk specimens of CNTs has been studied in the temperature range (4.2–293) K with use standard four-probe DC compensation technique. Electrical resistance also has been measured at temperature 77 and 293 K in magnetic field up to 2.2 T directed perpendicular to the current flowing through the specimen. Magnetoresistance has been defined as the ratio of the resistance change $\rho(B) - \rho(0)$ in the magnetic field to the resistance in the zero field $\rho(0)$: $\frac{\rho(B)-\rho(0)}{\rho(0)} = \frac{\Delta\rho}{\rho}$.

The measurements of thermopower have been made in the temperature range from 4.2 K up to 300 K. The specimens were cooled to a temperature of 4.2 K at a constant rate of 0.30 K/min. A temperature gradient (0.5–1.0 K) was created in the specimen and was measured with the help of a differential thermocouple Cu–CuFe (the sensitivity in the temperature range (4.2–30) K is (8–16) mcV/K). The measuring circuit was preliminarily calibrated with the superconducting ceramic YBaCuO which has a superconducting transition temperature $T_c = 80$ K and zero thermopower below T_c.

The error of the measurements did not exceed 0.5% for resistance and 1% for thermopower.

3 Results and Discussion

3.1 Resistivity of Modified SWCNTs

Figure 7 presents the temperature dependence of resistivity for bulk specimens of source and functionalized SWCNTs.

As it follows from the figure, for all specimens the character of resistivity temperature dependence is similar. At low temperature resistivity decreases sharply and then it is weakly dependent on temperature. However, the resistivity values themselves, as well as the ratio of resistivity at 4.2 K to resistivity at room temperature for specimens of modified SWCNTs, change significantly after modification. So, for the bulk specimen of modified SWCNTs #1, the values of resistivity at low temperatures become even slightly larger compared to the as-prepared SWCNTs. For bulk specimen of modified SWCNTs #3 resistivity at low temperature is somewhat lower, but only slightly. Therefore, for both these specimens, the ratio $\rho_{4.2}/\rho_r$ is close to this ratio in the as-prepared SWCNTs. Recall that both specimens (#1 and #3) were modified using 1,3diaminopropane as a functionalizing agent with minor differences

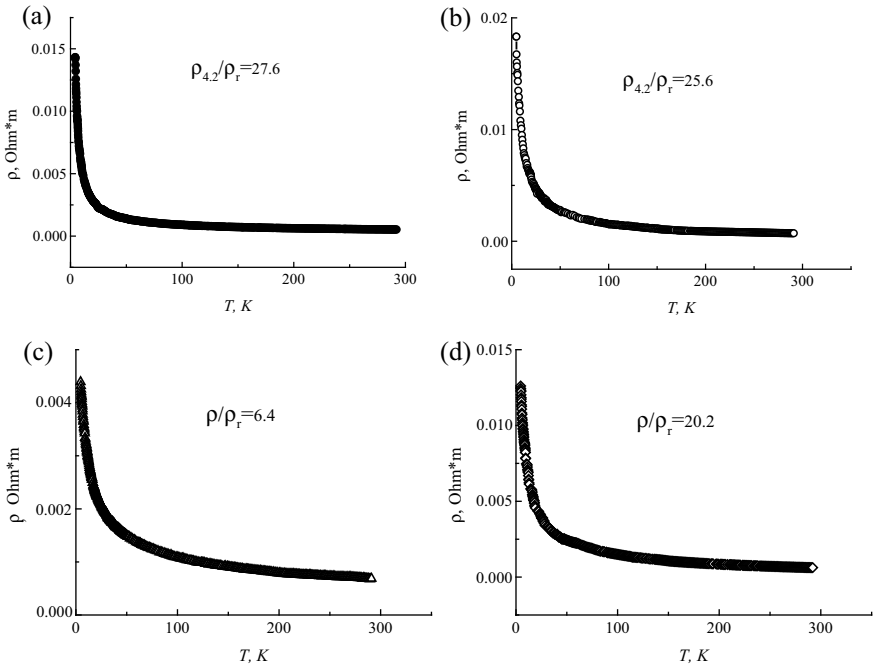

Fig. 7 Temperature dependences $\rho(T)$ for bulk specimens of as-prepared **a** and modified SWCNTs: **b** specimen #1, **c** specimen #2 and **d** specimen #3. The ratio of resistivity at 4.2 K and room temperature $\rho_{4.2}/\rho_{\mathrm{r}}$ for each specimen is indicated in the figures

in the modification process. On the other hand, significant changes in the value of low-temperature resistivity (almost three times) occur for specimen #2 of SWCNTs modified with the use of MEA as a functionalizing substance. That leads to a significant decrease of resistivity ratio $\rho_{4.2}/\rho_{293}$ from 26 for source SWCNTs to 6.3 for modified SWCNTs.

Let us consider possible conduction mechanisms for SWCNTs. The conductivity of a single-walled CNT is usually considered within the terms of a model of a one-dimensional Luttinger liquid of strongly interacting electrons. Within the framework of this model, there is a power-law temperature dependence of conductivity [16]:

$$\sigma(T) = aT^{\alpha}, \alpha = \frac{g + \frac{1}{g} - 2}{8}, \tag{2}$$

where a and α are the constants and α is related with Luttinger parameter g that characterizes the degree of charge carrier's interaction in the system. For defective SWCNTs, equation for conductivity takes on a more complex form [17–19]:

$$\sigma(T) = aT^{\alpha} + bT^{-1} + ce^{-\frac{T_l}{T+T_l}}. \tag{3}$$

In addition to (2), two more terms appear, which are responsible for the conductivity in the areas of possible branching of the CNT (second addition) and for conductivity through defective regions in the CNT (third addition). In the last addition T_1 is the temperature below which the barrier tunneling takes place and T_t is the temperature above which the thermo-activated conductivity above the barrier occurs. The ratio of terms in (3) depends on the degree of defectiveness of the specimen.

Real single-walled tubes are most often obtained in the form of mats or bundles, and to describe the conductivity of such systems in general, hopping conductivity model with variable hoping length for two-dimensional and three-dimensional cases is most often used [20, 21]. The general formula for hopping conductivity with the variable hopping length can be given as:

$$\sigma(T) = \sigma_0 \exp\left(-\left(\frac{T_0}{T}\right)^{\frac{1}{d}}\right), \tag{4}$$

where d is the dimensionality of the system, σ_0 and T_0 are the constants, and T_0 is inversely proportional to the length of localization.

The choice of the system dimensionality is determined by the structural features of the SWCNTs bulk specimens.

To identify possible mechanisms of conductivity for as-prepared SWCNTs, as well as for each specimen of modified SWCNTs, a detailed analysis of the conductivity temperature dependence has been carried out. The results of analysis are shown in Fig. 8. For each SWCNTs specimen, the figure shows the temperature dependence of conductivity in coordinates $\ln \sigma = f(T^{-1/4})$, which corresponds to the hopping mechanism of conductivity with a variable hoping length (3), and in coordinates $\ln \sigma = f(\ln T)$, which respectively corresponds to conductivity in the terms of model of a one-dimensional Luttinger liquid of strongly interacting electrons.

As it follows from presented dependences for as-prepared SWCNTs the main conductive mechanism is hopping with variable hopping lengths for the three-dimensional case. Such a conductivity mechanism is usually the main one precisely for the as-prepared SWCNTs, which are obtained in the form of mats or felt and which contain, in addition to CNTs, a sufficient number of disordered carbon particles [22–24]. Also, this conductivity mechanism is typical for disordered graphite, in particular so-called amorphous carbon. The characteristic temperature T_0 determined from the dependence $\ln \sigma = f(T^{-1/4})$ equals to 2902 K. This value of characteristic temperature T_0 is much larger than corresponding value T_0 for mats of SWCNTs in [21], but close to value T_0 for amorphous carbon in [25].

As can be seen from the figures above, modification of SWCNTs by cobalt-containing complexes did not lead to a dramatic change in the conductivity of the

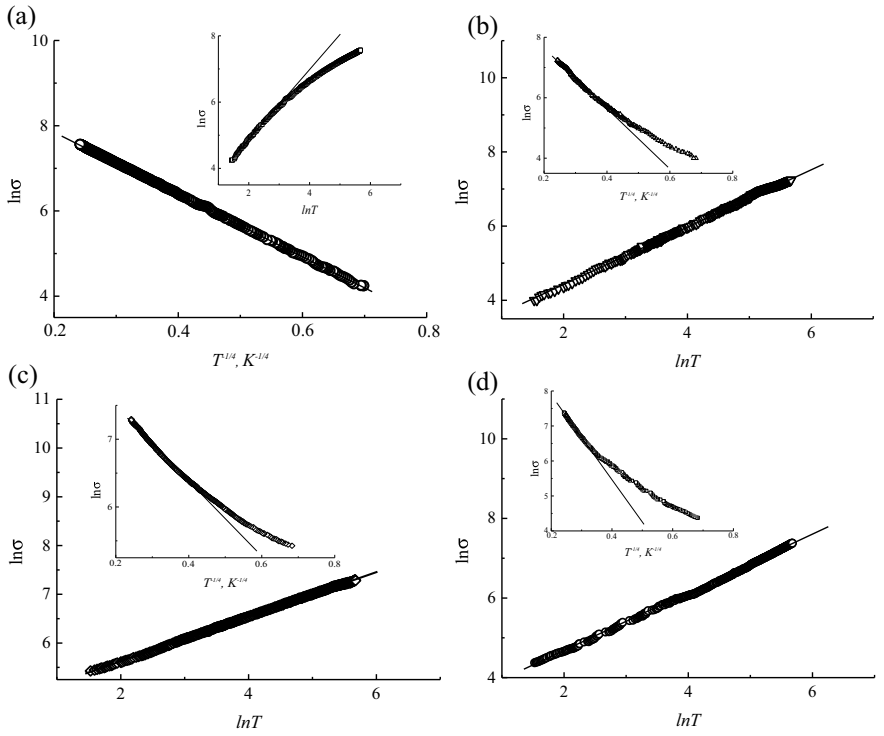

Fig. 8 Temperature dependences of conductivity for bulk specimens of as-prepared **a** and modified, **b** specimen #1, **c** specimen #2 and **d** specimen #3 SWCNTs in coordinates $\ln \sigma = f(T^{-1/4})$ (**b**, **c**, and **d**—inset) and in coordinates $\ln \sigma = f(\ln T)$ (**a**—inset)

CNTs bulk specimens. However, such modification significantly affected the character of the temperature dependence of conductivity for these specimens. For all specimens of modified SWCNTs conductivity temperature dependence is well described in the terms of power temperature law that is typical for individual SWCNTs (1).

In Table 1, calculated from dependence $\ln \sigma = f(\ln T)$, parameters of conductivity for bulk specimens of modified SWCNTs are presented.

As can be seen from Table 1, for specimens of modified SWCNTs #1 and #3, for which the conductivity does not change significantly after modification, the values of the coefficient α are close, while for specimen of modified SWCNTs #2, for which the conductivity increases after modification, the value of α is almost two

Table 1 Calculated parameters α, g and a for modified SWCNTs

Specimen	α	g	a, S/m
#1	0.79	0.12	16.6
#2	0.46	0.18	110.0
#3	0.73	0.13	23.6

times smaller. However, the values of parameter g for all specimens are close and indicate the formation in the modified SWCNTs of a one-dimensional system of strongly interacting electrons. Let us dwell on this moment in more detail. As is known for pressed specimens, the total resistance R is determined as sum of two additions: $R = R_{CNT} + r_C$, where R_{CNT} is the resistance of separate CNTs and r_C is the contact resistance between tubes. The contact resistance r_C depends on many factors among them surface condition, size of contact spot and contact pressure. Since bulk-pressed specimens have been obtained without a binder, the contact between individual tubes is direct, without a layer of polymer. A change in the conductivity of a bulk specimen after modification can be associated with a change in the conductivity of the tubes R_{CNT} and with a change in the contact resistance r_C between them, as well as these two processes simultaneously. Indeed, the functionalization and modification of the CNTs' surface can both reduce the conductivity of individual CNTs due to the destruction of the graphite layer π-system and increase it due to charge redistribution as a result of the attachment of functional groups to the CNT surface. The contact resistance between the separate tubes usually increases after functionalization and modification due to the appearance of a small negative charge on the surface of functionalized CNTs caused by the attachment of functional groups to the tubes surface. In addition, treatment of CNTs with acid solutions provides to remove disordered carbon particles from the primary networks of as-prepared SWCNTs, which usually have a developed surface and serve as a peculiar «bridges» between individual CNTs, increasing their contact surface.

Thus, it is the change in the character of the temperature dependence of the conductivity of the SWCNTs bulk specimens after chemical treatment indicates that the SWCNTs surface has been modified.

3.2 Magnetoresistance of Modified SWCNTs

Figure 9 presents the dependence of magnetoresistance $\frac{\Delta\rho}{\rho}$ on magnetic field for as-prepared SWCNTs at room temperature and $T = 77$ K.

As it is seen from the figure, magnetoresistance is symmetrical with respect to the direction of the magnetic field. At room temperature, the magnetoresistance is positive, and its values do not exceed 0.035% at the maximum magnetic field of measurement. When the temperature decreases, the magnetoresistance changes its sign, while the absolute value of the magnetoresistance increases to 0.15% in the maximum measurement field.

For materials in which the hopping conduction mechanism is implemented, the effect of compression of the wave function of the localized state in the magnetic field takes place in the magnetoresistance [26–29]. According to this mechanism, within the limits of weak magnetic fields ($\xi < l_B$), the magnetoresistance is described by the expression:

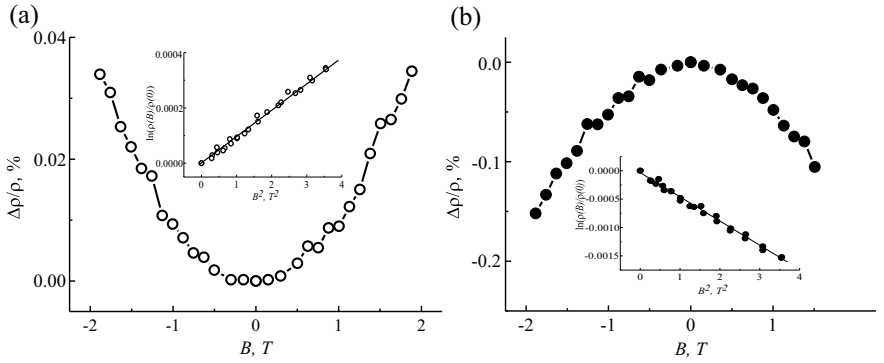

Fig. 9 Dependence $\frac{\Delta\rho}{\rho}(B)$ for bulk specimen of as-prepared SWCNTs at room temperature (**a**) and T = 77 K (**b**). Corresponding dependences in coordinates $\ln\left(\frac{\rho(B)}{\rho(0)}\right) = f\left(B^2\right)$ are shown in the inset

$$ln\left(\frac{\boldsymbol{\rho(B)}}{\boldsymbol{\rho(0)}}\right) = t_d\left(\frac{\xi}{l_B}\right)^4\left(\frac{T_0}{T}\right)^{3\alpha}, \tag{5}$$

where ξ is the wave function localization radius, l_B is the magnetic length, $l_B = \sqrt{\frac{h}{2\pi eB}}$, t_d and α are the numerical coefficients, and T_0 is the characteristic temperature.

So, implementation of the mechanism of compression of the localized state wave function in the magnetic field in disordered systems involves a positive magnetoresistance that depends quadratically on the magnetic field. However, as can be seen from Fig. 9, as the temperature decreases, the magnetoresistance of as-prepared SWCNTs becomes negative. Therefore, to describe the magnetoresistance of as-prepared SWCNTs, it is not enough to consider only the model of the wave function compression in a magnetic field [29]. As shown in works [30, 31], the negative component of the magnetoresistance can be related to the implementation in carbon materials of the spin-polarized magnetoresistance mechanism [31].

The spin-polarized mechanism of magnetoresistance leads to the following magnetoresistance expression in the region of a weak magnetic field [30]:

$$ln\left(\frac{\rho(B)}{\rho(0)}\right) = \alpha A\left(\frac{T_0}{T}\right)^{\alpha}\left(\frac{\mu B}{k_b T}\right)^2, \tag{6}$$

where μ is the effective magnetic moment of an electron and A is the some parameter that is related to the relationship between concentrations and localization radii of localized states.

Thus, it follows from (5) and (6) that both mechanisms of magnetoresistance are quadratic with respect to magnetic induction within weak magnetic fields

$$\ln\left(\frac{\rho(B)}{\rho(0)}\right) = \left[t_{\mathrm{d}}\left(\frac{2e^2}{h}\right)^2\left(\frac{T_0}{T}\right)^{3\alpha} + \alpha A\left(\frac{T_0}{T}\right)^{\alpha}\left(\frac{\mu}{k_b T}\right)^2\right]B^2. \tag{7}$$

The sign of the magnetoresistance will be determined by the ratio between the contributions of two magnetoresistance mechanisms, the mechanism of the compression of the localized charge carriers wave function and the spin–orbit mechanism.

In Fig. 9, the insets show the dependences $\ln\left(\frac{\rho(B)}{\rho(0)}\right) = f\left(B^2\right)$ for as-prepared SWCNTs at two temperatures. As can be seen from the figure, the dependence $\ln\left(\frac{\rho(B)}{\rho(0)}\right) = f\left(B^2\right)$ is linear at both temperatures. Change of magnetoresistance signs at different temperatures indicates the change of primary mechanisms of magnetoresistance in different temperature ranges. At room temperature, the compression mechanism of the wave function of localized charge carriers is prevailing. When the temperature decreases, the spin-orbital magnetoresistance makes a more significant contribution to the magnetoresistance, which causes changes in the sign of the magnetoresistance.

Figure 10 shows the dependences $\frac{\Delta\rho}{\rho}(B)$ for bulk specimens of modified by cobalt-containing complexes SWCNTs (specimens #2 and #3) at two temperatures: $T =$ 293 K and $T = 77$ K.

As it is follows from the figures, the character of the temperature and field dependences of magnetoresistance for both specimens of modified SWCNTs changes significantly compared to the as-prepared SWCNTs. For both specimens of modified SWCNTs, the magnetoresistance is negative at room temperature and at a temperature of 77 K. As the temperature decreases, the absolute value of the magnetoresistance for both specimen increases. However, the absolute values of magnetoresistance for specimen #2 are approximately 10 times smaller compared to the absolute values of magnetoresistance for specimen #3. In addition, as can be seen from the figure, for both specimens of modified SWCNTs at $T = 77$ K, with increasing magnetic

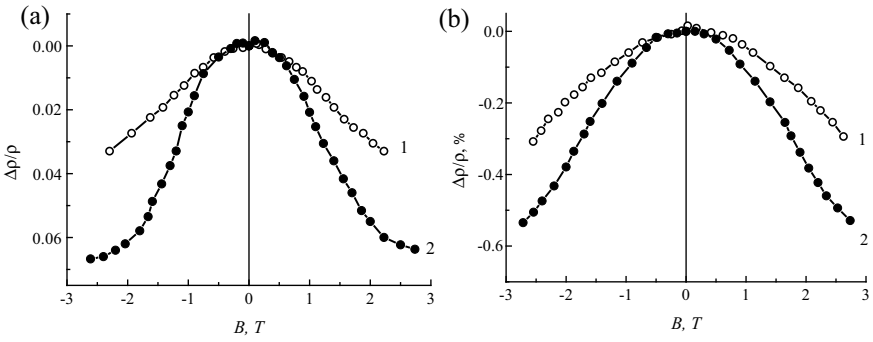

Fig. 10 Dependences $\frac{\Delta\rho}{\rho}(B)$ for bulk specimens of modified SWCNTs (#2 (**a**) and #3 (**b**)) at $T =$ 293 K (curve 1) and $T = 77$ K (curve 2)

field the deviations from the quadratic dependence of the magnetoresistance on the magnetic field are observed.

Let us consider in more detail the mechanisms of magnetoresistance for modified SWCNTs. As was shown above, the temperature dependence of conductivity for modified SWCNTs is described by a power law, which is characteristic for one-dimensional conductors. Moreover, the values of the power exponent are close to the corresponding values of the power exponent within the terms of the conduction model of a one-dimensional Luttinger liquid of strongly interacting electrons. As it is known, for CNTs of a perfect structure, the conductivity of which is considered within the terms of a two-dimensional model, a negative magnetoresistance associated with the manifestation of the charge carriers' weak localization effect is observed. Let us evaluate whether the negative magnetoresistance for modified SWCNTs can be a manifestation of the effect of charge carriers' weak localization, but for a one-dimensional system.

As is well known weak localization occurs as a result of the interference of direct and elastically scattered electron waves on inhomogeneities of the system. For one-dimensional system, conductivity in magnetic field taking into account the additive due to weak localization is given by equation [32, 33]

$$\Lambda(B) = \Lambda_0 - \frac{2e^2}{hL}\left(\frac{1}{L_\varphi^2} + \frac{e^2B^2w^2}{3\hbar}\right)^{-\frac{1}{2}}, \tag{8}$$

where $\Lambda(B)$ is the conductivity in magnetic field B, Λ_0 is classical Drude conductance without the localization addition, L_φ is the coherence length of the wave function, and L and w, respectively, the length and diameter of the nanotube. Note that (8) is valid only for case $L_\varphi > w$. In the absence of a magnetic field, the conductivity can be written as

$$\Lambda(0) = \Lambda_0 - \frac{2e^2L_\varphi}{hL}. \tag{9}$$

Let us find the difference between conductivities in a magnetic field and in the absence of a magnetic field

$$\Lambda(\mathrm{B}) - \Lambda(0) = \frac{2e^2L_\varphi}{hL}\left[1 - \frac{\sqrt{3}\hbar}{\sqrt{3\hbar^2 + L_\varphi^2e^2B^2w^2}}\right]. \tag{10}$$

Accordingly, the difference between specific conductivities in a magnetic field $\sigma(B)$ and in the absence of a magnetic field $\sigma(0)$ has the form

$$\sigma(B) - \sigma(0) = \Delta\sigma(B) = \frac{8e^2L_\varphi}{\pi w^2h}\left[1 - \frac{\sqrt{3}\hbar}{\sqrt{3\hbar^2 + L_\varphi^2e^2B^2w^2}}\right] \tag{11}$$

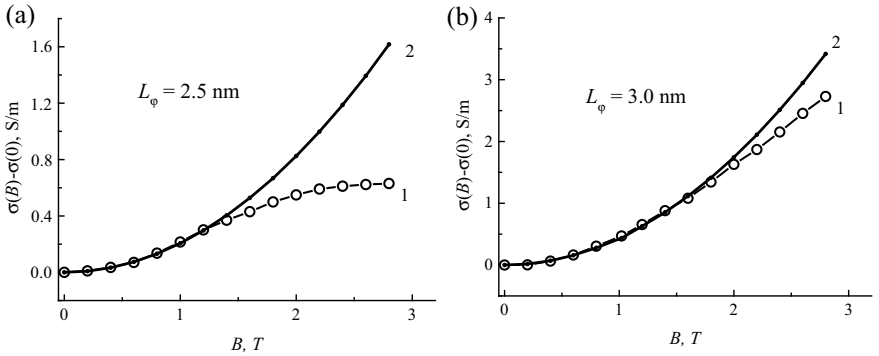

Fig. 11 Experimental (1) and calculated by (10) (2) dependences of specific conductivity on magnetic field for specimens of modified SWCNTs #2 (**a**) and #3 (**b**). The values of the fitting parameter L_φ are indicated in the figure

Equation (11) contains only one unknown parameter L_φ which was fitted.

The obtained experimental dependences $\Delta\sigma(B)$ as well as calculated by (11) using the fitting parameter for both specimens of modified SWCNTs are shown in Fig. 11.

As can be seen from the figure, the best match between the calculated dependence $\Delta\sigma(B)$ and the experimental one for SWCNTs with a fixed diameter $w = 1.4$ nm is observed at the values of the fitting parameter L_φ, 2.5 nm for specimens #2 and 3 nm for specimen #3, respectively. Note that condition $L_\varphi > w$ is fulfilled. However, the coincidence is observed not in the entire interval of the magnetic field in which the measurements have been carried out, but only when $B < 1.3$ T for specimen #2 and for $B < 1.7$ T for specimen #3.

Thus, it can be assumed that the positive conductivity in the magnetic field for specimens of modified SWCNTs below the specified magnetic fields is associated with the manifestation of the effect of charge carriers' weak localization for a one-dimensional system.

3.3 Thermopower of Modified SWCNTs

Measurements of thermopower temperature dependence $S(T)$ have been carried out for as-prepared SWCNTs in temperature interval from 77 K up to 293 K and for modified SWCNTs (specimen #2) in temperature interval from 4.2 K up to 293 K. The results of measurements are presented in Fig. 12.

As can be seen from the figure, for as-prepared SWCNTs the linear temperature dependence of thermopower is observed. For modified SWCNTs there is linear dependence of thermopower on temperature at low and high temperatures. However, in the temperature interval from ~ 50 K up to 250 K significant deviation from linear dependence occurs.

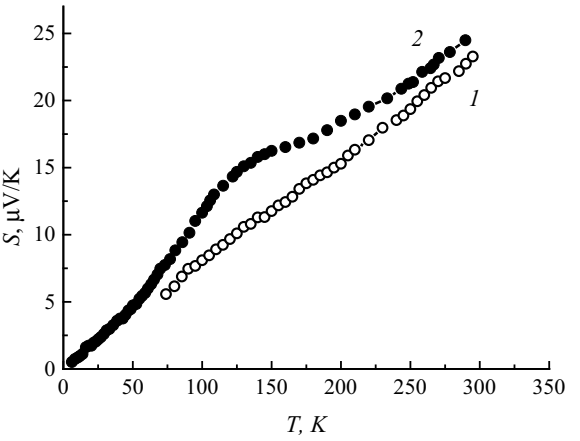

Fig. 12 Temperature dependences of thermopower $S(T)$ for as-prepared SWCNTs (1) and for SWCNTs modified with cobalt-containing complexes (2)

As is known, thermopower is very sensitive to the features of the band structure of the material, its electronic and phonon spectrum, as well as to the scattering mechanisms of charge carriers and phonons.

For graphite materials with a perfect structure, the dependence of thermopower on temperature has a very complex form. Such dependence of thermopower on temperature is caused by two factors. First, thermopower is determined by the contribution of two components: diffuse thermopower and thermopower associated with phonon drag effect. The phonon drag effect leads to the appearance of additional thermopower, caused by additional charge carriers dragged from the hot specimen end to the cold end by phonon flux via momentum transfer. Secondly, diffuse thermopower for graphite with a perfect structure, which has two types of main charge carriers with equal concentration, is characterized by a complex, nonlinear temperature dependence. However, the situation changes significantly for defective graphite materials. For such materials, the temperature of maximum the phonon drag effect shifts to low temperatures, and the magnitude of the effect itself becomes very small. As for the diffuse thermopower, it acquires a linear dependence on temperature under conditions of predominant hole conductivity. This temperature dependence of thermopower is typical for metals. So, metallic diffusion thermopower can be written as

$$S_{\mathrm{d}} = \frac{\pi^2 k_{\mathrm{b}}^2 T}{3eE_{\mathrm{F}}}(1-p), \tag{12}$$

where E_{F} is the Fermi energy and p is the coefficient associated with the prevailing charge carriers scattering mechanism. Similar temperature dependences of thermopower were observed both for SWCNTs' mats and for individual SWCNTs in a number of papers.

Modification of as-prepared SWCNTs with cobalt-containing complexes leads to a change in the temperature dependence of the thermopower, namely to a deviation

from the linear dependence in the temperature interval of (50–250) K. At the same time, the values of thermopower at low and high temperatures almost coincide with the corresponding values of thermopower for unmodified SWCNTs.

Figure 13 presents the difference between the experimental values of the thermopower S_{exp} and the linear approximation $S_d = cT$ (12).

As it follows from the figure, the curve $S_{exp} - S_d$ has the form of a broad band with a maximum at temperature ~ 130 K. Similar deviations from the linear dependence $S(T)$ have been observed for SWCNTs in a number of studies. However, in the literature, there is no single view on the nature of such a deviation from linear dependence. Several effects that could lead to such behavior have been discussed in the literature. In [34] thermopower is considered as sum of a linear metallic term and an exponentially weighted $T^{1/2}$ variable range hopping term that reflects the "freezing-out" of semiconducting contributions at low temperatures. For doped SWCNTs, the nonlinearity in thermopower is associated with the appearance of localized states near the Fermi level due to the introduction of boron or nitrogen atoms into the CNTs wall structure. Another reason that can lead to the deviation of thermopower from a linear dependence is the Kondo effect. The thermopower investigations on SWCNTs mats in [35] suggest that the observed giant thermopower comes from the contributions of Kondo state induced by magnetic transition-metal impurities. For the investigated SWCNTs, the cobalt ion is contained in the composition of complexes, and cobalt does not present as individual particles. Obviously, for these SWCNTs, the Kondo effect cannot cause deviation of the thermopower from the linear dependence.

In the [36] the authors assume that the origin of the deviation of the thermopower temperature dependence from the linear one is the manifestation of the effect of phonon drag of charge carriers. The carried-out calculations by Scarola and Mahan in [37] show that the phonon drag thermopower in SWCNTs increases rapidly with T at low temperatures and approaches approximately a constant for $T > 100$ K. So, the thermoelectric power of the SWCNTs can be considered as sum of a linear diffusion

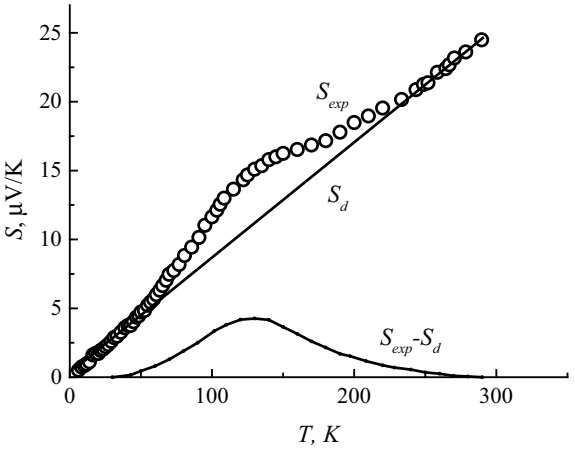

Fig. 13 Difference between the experimental values of the thermopower S_{exp} and the linear approximation $S_d = cT$

thermopower S_d and phonon drag thermopower, which is approximately constant for temperature interval from 110 K up to 300 K.

Really, the shape of the dependence $(S_{exp} - S_d) = f(T)$ is similar to the temperature dependence of the phonon drag thermopower, which is observed in acceptor intercalated compounds based on fine crystalline graphite. The temperature at which the maximum in the dependence $(S_{exp} - S_d) = f(T)$ occurs also coincides with the temperature of the phonon drag thermopower maximum.

Let us estimate the value of the Fermi energy E_F from the linear section of the dependence $S(T)$ (Fig. 13) using (12). The calculated value of E_F is 0.29 eV. The corresponding value of the Fermi wave vector is $k_F = 4.5 \times 10^8$ m^{-1}.

Let us determine the temperature at which the maximum effect of phonon capture of charge carriers occurs, using the formula

$$T_{max} = \frac{2\hbar v_s k_F}{k_b}, \tag{13}$$

where v_s is the sound speed and $v_s = 2.1 \times 10^4$ m/s as for monocrystalline graphite. According to calculation $T_{max} = 140$ K, which correlates well with the value of the temperature $T_{max\ exp} = 130$ K, at which a maximum in the dependence $(S_{exp} - S_d) = f(T)$ is observed.

Thus, the carried-out studies of thermopower revealed that for the as-prepared SWCNTs, thermopower has a linear dependence on temperature and is determined only by the diffuse component of thermopower, while for modified SWCNTs, two mechanisms contribute to thermopower, namely diffuse thermopower and thermopower caused by phonon drag of charge carriers.

3.4 Discussion

The results of research into the transport properties of SWCNTs surface-modified with cobalt-containing complexes allow to assume that these modified SWCNTs can be considered as one-dimensional conductors, and such one-dimensionality of transport properties is preserved in bulk pressed specimens of modified SWCNTs.

The as-prepared SWCNTs are considered as 3D system. This is explained by the fact that, on the one hand, SWCNTs are contained in the source carbon nanomaterial in the form of mats, bundles of very tangled tubes. On the other hand, the source carbon nanomaterial contains a sufficiently large amount of disordered carbon phase, in other words, amorphous nanocarbon particles with a developed surface. The presence in specimen a significant amount of amorphous nanocarbon particles causes a significant decrease of contact resistance between individual nanotubes. The amorphous nanocarbon particles with a sufficiently developed surface promote the adhesion of individual CNTs to each other. It is the presence of large number of disordered carbon phase that allows to obtain bulk specimens of SWCNTs without

the use of a binder. Thus, bulk specimen of as-prepared SWCNTs can be considered as 3D system.

Let us analyze the changes in the structural and phase composition of the source carbon nanomaterial and the surface morphology of the as-prepared SWCNTs in the process of their modification with cobalt-containing complexes. On the first stage the treatment of the source SWCNTs with hydrogen peroxide results in formation of a significant number of broken bonds. At the next stage as-prepared SWCNTs are treated with water solution of hydrochloric acid that leads to the removal from the SWCNT's strands of metal catalyst and amorphous nanocarbon. Then CNTs surface is functionalized by methods of non-covalent functionalization, and cobalt-containing complexes can join to carbon atoms at the CNTs surface through functional groups. So, treatment of as-prepared SWCNTs leads to the removal of amorphous nanocarbon particles and contributes to the disentanglement of CNTs. It was these two factors that ensured the "three-dimensionality" of the bulk specimens of the as-prepared SWCNTs. In addition, as is known, a small localized negative charge appears on the SWCNT surface as a result of functionalization. This also creates conditions that prevent the movement of charge carriers between the individual tubes.

Thus, all the given facts indicate that after the proposed treatment of as-prepared SWCNTs, the contact resistance between the individual CNTs in the bulk specimen has increased significantly. Therefore, the charge carriers in the bulk specimen can move only along each tube, and charge transfer between individual CNTs is unlikely. Thus, in the bulk specimens of SWCNTs, the conductivity mechanism is formed, which is characteristic for the 1D systems. This situation in the bulk specimens of SWCNTs can be compared with the processes that occur at the formation of graphite intercalation compounds (GICs). Graphite intercalation compounds are layered structures in which layers of graphite (their number S determines the stage of the GICs) and monomolecular or monoatomic layers of other substances called intercalates alternated. The condition for the formation of GICs is the transfer of charge from the intercalates layers to the graphite layers, which results in an increase in the concentration of free charge carriers in the graphite layers. At the same time intercalates layers form an electrostatic barrier from the charges localized on them. Due to this the charge carriers in the GICs can move only along the graphite layers, forming a two-dimensional electronic system. And GICs are considered as two-dimensional conducting systems which two-dimensionality is caused not by their geometrical sizes and is connected with features of their electronic structure.

Thus, it can be assumed that the "one-dimensionality" of the transport properties of modified SWCNTs bulk specimens can be explained by the features of the zone structure of SWCNTs modified with cobalt-containing complexes. The concentration of a small negative charge on the CNT surface and, obviously, the enrichment of the CNT with an additional positive charge lead to the formation of one-dimensional system in the bulk specimen, which is not related to the geometric dimensions and shape of the bulk conductor, but is caused by the peculiarities of the zone structure of individual modified SWCNT.

4 Conclusion

Thus, the carried-out investigations of structural and phase composition of modified SWCNTs have revealed that all proposed modification schemes allow to obtain SWCNTs modified on the surface by cobalt-containing complexes.

The studies of the resistivity temperature and magnetic field dependences have shown that for bulk specimens of as-prepared SWCNTs the main mechanism of conductivity is the 3D hopping mechanism with the variable hopping length. This conduction mechanism is typical for disordered graphite materials, as well as for mats and binders of SWCNTs. Magnetoresistance of as-prepared SWCNTs is caused by two mechanisms. The first of them is the mechanism of compression of the wave function of localized charge carriers that leads to positive magnetoresistance. The second mechanism is spin-orbital, which causes the change in the sign of the magnetoresistance. The thermopower of as-prepared SWCNTs has only a linear dependence on temperature.

Modification of SWCNTs by surface with cobalt-containing complexes results into a change in the character of the conductivity of SWCNTs specimens. For modified SWCNTs the bulk specimens' conductivity is described in the terms of power temperature law that is typical for individual SWCNTs. Moreover, the negative magnetoresistance observed for modified SWCNTs at low temperatures is related with the manifestation of the effect of charge carriers' weak localization for a one-dimensional system. Thermopower of modified with cobalt-containing complexes SWCNTs contains two additions. One of them is the diffuse thermopower, and other is the phonon drag thermopower.

Thus, when modifying the SWCNTs' surface with cobalt-containing complexes, a transition from a three-dimensional system to a one-dimensional system occurs. Such transition from a three-dimensional system for bulk specimen of as-prepared SWCNTs to a one-dimensional system for bulk specimen of modified SWCNTs is due to a change in both the structural and phase composition of the source carbon nanomaterial and a change in the state of the SWCNTs' surface as a result of modification. Surface modification of SWCNTs leads to the creation on the surface of CNTs small localized negative charge which acts as an electrostatic screen. The presence of such a charge makes it impossible to transfer charge between individual tubes and promotes the formation of a 1D conductive system of SWCNTs.

References

1. R. Andrews, M.C. Weisenberger, Carbon nanotube polymer composites. Solid State Mater. Sci. **8**, 31–37 (2004). https://doi.org/10.1016/j.cossms.2003.10.006
2. J. Yun, J.S. Im, Y.-S. Lee, H.-I. Kim, Effect of oxyfluorination on electromagnetic interference shielding behavior of MWCNT/PVA/PAAc composite microcapsules. Eur. Polym. J. **46**, 900–909 (2010). https://doi.org/10.1016/j.eurpolymj.2010.02.005

3. J. Zhang, H. Zou, Q. Qing, Y. Yang, Q. Li, Z. Liu, X. Guo, Z. Du, Effect of chemical oxidation on the structure of single-walled carbon nanotubes. J. Phys. Chem. B **107**, 3712–3718 (2003). https://doi.org/10.1021/jp027500u
4. M.N. Tchoul, W.T. Ford, G. Lolli, D.E. Resasco, S. Arepalli, Effect of mild nitric acid oxidation on dispersability, size, and structure of single-walled carbon nanotubes. Chem. Mater. **19**, 5765–5772 (2007). https://doi.org/10.1021/cm071758l
5. A.B. Sulong, N. Muhamad, J. Sahari, R. Ramli, B.M. Deros, J. Park, Electrical conductivity behaviour of chemical functionalized MWCNTs epoxy nanocomposites. Eur. J. Sci. Res. **29**, 13–21 (2009)
6. S.A.V. Jannuzzi, B. Martins, L.E.S.C. Huamaní, A.L.B. Formiga, Supramolecular approach to decorate multi-walled carbon nanotubes with negatively charged iron(II) complexes. J. Braz. Chem. Soc. **28**, 2–10 (2017). https://doi.org/10.5935/0103-5053.20160137
7. S.M. Alshehri, T. Ahamad, A. Aldalbahi, N. Alhokbany, Pyridylimine cobalt(II) and nickel(II) complex functionalized multiwalled carbon nanotubes and their catalytic activities for ethylene oligomerization. Adv. Polym. **35**, 21528.1–21528.10 (2016). https://doi.org/10.1002/adv.21528
8. V. Yu Evtushok, I.D. Ivanchikova, O. Yu Podyacheva, O.A. Stonkus, A.N. Suboch, Yu.A. Chesalov, O.V. Zalomaeva, O.A. Kholdeeva, Carbon nanotubes modified by Venturello complex as highly efficient catalysts for alkene and thioethers oxidation with hydrogen peroxide. Front. Chem. **7**, 858 (2019). https://doi.org/10.3389/fchem.2019.00858
9. S. Gómez-Coca, E. Ruiz, Magnetic behaviour of transition metal complexes with functionalized chiral and C_{60}-filled nanotubes as bridging ligands: a theoretical study. Magnetochemistry **1**, 62–71 (2015). https://doi.org/10.3390/magnetochemistry1010062
10. W. Orellana, Metal-phthalocyanine functionalized carbon nanotubes as catalyst for the oxygen reduction reaction: a theoretical study. Chem. Phys. Lett. **541**, 81–84 (2012). https://doi.org/10.1016/j.cplett.2012.05.048
11. S. Banerjee, S.S. Wong, Functionalization of carbon nanotubes with a metal-containing molecular complex. Nano Lett. **2**, 49–53 (2002). https://doi.org/10.1021/nl010070j
12. S. Arumugam, L.D. Chakkarapani, Metal nanoparticles functionalized carbon nanotubes for efficient catalytic application. Mater. Res. Express **6**(10), 50e3 (2019). https://doi.org/10.1088/2053-1591/ab42ff
13. A. Oki, L. Adams, Z. Luo, E. Osayamen, P. Biney, V. Khabashesku, Functionalization of single-walled carbon nanotubes with N-[3-(trimethoxysilyl)propyl]ethylenediamine and its cobalt complex. J. Phys. Chem. Solids **69**, 1194–1198 (2008). https://doi.org/10.1016/j.jpcs.2007.10.129
14. I.V. Ovsiienko, L. Yu Matzui, M.I. Zakharenko, N.G. Babich, T.A. Len, Yu.I. Prylutskyy, D. Hui, Yu.M. Strzhemechny, P.C. Eklund, Magnetometric studies of catalyst refuses in nanocarbon materials. Nanoscale Res. Lett. **3**, 60–64 (2008). https://doi.org/10.1007/s11671-007-9115-z
15. I.V. Ovsiienko, T.A. Len, L.Yu. Matzui, O.A. Golub, Yu.I. Prylutskyy, T.L. Tsaregradskaya, G.V. Saenko, The structure and transport properties of single-walled carbon nanotubes modified by cobalt-containing complexes. J. Nano Electron. Phys. **12**, 06023–1–06023–7 (2020). https://doi.org/10.21272/jnep.12(6).06023
16. M. Bockrath, D.H. Cobden, J. Lu, A.G. Rinzler, R.E. Smalley, L. Balents, P.L. McEuen, Luttinger-liquid behaviour in carbon nanotubes. Nature **397**, 598–601 (1999)
17. D.J. Bae, K.S. Kim, Y.S. Park, E.K. Suh, K.H. An, J.-M. Moon, S.C. Lim, S.H. Park, Y.H. Jeong, Y.H. Lee, Transport phenomena in an anisotropically aligned single-wall carbon nanotube film. Phys. Rev. B **64**, 233401–233411 (2001). https://doi.org/10.1103/PhysRevB.64.233401
18. M. Shiraishi, M. Ata, Conduction mechanisms in single-walled carbon nanotubes. Synth. Met. **128**, 235–239 (2002). https://doi.org/10.1016/S0379-6779(02)00013-9
19. A.B. Kaiser, G.U. Flanagan, D.M. Stewart, D. Beaglehole, Heterogeneous model for conduction in conducting polymers and carbon nanotubes. Synth. Met. **117**, 67–73 (2001). https://doi.org/10.1016/S0379-6779(00)00540-3
20. B. Liu, B. Sundqvist, O. Andersson, T. WaÊgberg, E.B. Nyeanchia, X.-M. Zhu, G. Zou, Electric resistance of single-walled carbon nanotubes under hydrostatic pressure. Solid State Commun. **118**, 31–36 (2001). https://doi.org/10.1016/S0038-1098(01)00034-5

21. I.V. Ovsiyenko, T.A. Len, L.Yu. Matzui, Yu.I. Prylutskyy, U. Ritter, P. Scharff, F. Le Normand, P. Eklund, Resistance of a nanocarbon material containing nanotubes. Molecular Cryst. Liquid Cryst. **468**, 289/[641]–297[649] (2007). https://doi.org/10.1080/15421400701231582
22. Y. Yosida, I. Oguro, Variable range hopping conduction in bulk samples composed of single-walled carbon nanotubes. J. Appl. Phys. **86**, 999 (1999). https://doi.org/10.1063/1.370838
23. R. Gaa, J.-P. Salvetat, L. Forro, Pressure dependence of the resistivity of single-wall carbon nanotube ropes. Phys. Rev. B **61**, 7320 (2000). https://doi.org/10.1103/PhysRevB.61.7320
24. M.S. Fuhrer, W. Holmes, P.L. Richards, P. Delaney, S.G. Louie, A. Zettl, Nonlinear transport and localization in single-walled carbon nanotubes. Synth. Met. **103**, 2529–2532 (1999). https://doi.org/10.1016/S0379-6779(98)00305-1
25. L. Matzui, L. Vovchenko, I. Ovsienko, Thermopower of pregraphitic carbons. Mol. Cryst. Liquid Cryst. **340**, 361–366 (2000). https://doi.org/10.1080/10587250008025493
26. G.T. Kim, E.S. Choi, D.C. Kim, D.S. Suh, Y.W. Park, K. Liu, G. Duesberg, S. Roth, Magnetoresistance of an entangled single-wall carbon-nanotube network. Phys. Rev. B **58**, 16064–16069 (1998). https://doi.org/10.1103/PhysRevB.58.16064
27. V.A. Samuilov, J. Galibert, V.K. Ksenevich, V.J. Goldman, M. Rafailovich, J. Sokolov, I.A. Bashmakov, V.A. Dorosinets, Magnetotransport in mesoscopic carbon networks. Physica B **294–295**, 319–323 (2001). https://doi.org/10.1016/S0921-4526(00)00668-2
28. S.V. Demyshev, A.A. Pronin, N.E. Sluchanko, N.A. Samarin, A.G. Lyapin, V.V. Brazhkin, T.D. Varfolomeeva, S.V. Popova, 1D-3D crossover in the hopping conductivity of carbines. Lett. JETP **72**, 547–552 (2000) (in Russian)
29. M.E. Raikh, J. Czingon, F. Koch, W. Schoepe, K. Ploog, Mechanisms of magnetoresistance in variable-range-hopping transport for two-dimensional electron systems. Phys. Rev. B **45**, 6015–6022 (1992). https://doi.org/10.1103/PhysRevB.45.6015
30. S.V. Demyshev, A.D. Bozhko, V.V. Glushkov, E.A. Kataeva, A.G. Lyapin, E.D. Obraztsova, T.V. Ishchenko, N.A. Samarin, Scaling of magnetoresistance of carbon nanomaterials in the region of Mott type hopping conductivity. FTT **50**, 1332–1337 (2008). (in Russian)
31. S.V. Demyshev, A.A. Pronin, Magnetoresistance of carbon nanomaterials. FTT **48**, 1285–1294 (2006). (in Russian)
32. B.L. Altshuler, A.G. Aronov, D.E. Khmelnitzky, Effects of electron-electron collisions with small energy transfers on quantum localization. J. Phys. C Solid State Phys. **15**, 7367 (1982). https://doi.org/10.1088/0022-3719/15/36/018
33. C.W.J. Beenakker, H. van Houten, Boundary scattering and weak localization of electrons in a magnetic field. Phys. Rev. B **38**, 3232 (1988). https://doi.org/10.1103/PhysRevB.38.3232
34. Y.-M. Choi, D.-S. Lee, R. Czerw, P.-W. Chiu, N. Grobert, M. Terrones, M. Reyes-Reyes, H. Terrones, J.-C. Charlier, P.M. Ajayan, S. Roth, D.L. Carroll, Y.-W. Park, Nonlinear behavior in the thermopower of doped carbon nanotubes due to strong, localized states. Nano Lett. **3**, 839–842 (2003). https://doi.org/10.1021/nl034161n
35. F. Xu, J.-L. Zhu, Conductance and thermoelectric power in carbon nanotubes with magnetic impurities. Mesoscale Nanoscale Phys. (2007). arXiv:cond-mat/0703373 [cond-mat.mes-hall]. https://doi.org/10.48550/arXiv.cond-mat/0703373
36. C. Yu, L. Shi, Z. Yao, D. Li, A. Majumdar, Thermal conductance and thermopower of an individual single-wall carbon nanotube. Nano Lett. **5**, 1842–1846 (2005). https://doi.org/10.1021/nl051044e
37. V.W. Scarola, G.D. Mahan, Phonon drag effect in single-walled carbon nanotubes. Phys. Rev. B. **66**, 205405 (2002). https://doi.org/10.1103/PhysRevB.66.205405